J Geod (2014) 88:625–642
DOI 10.1007/s00190-014-0710-3

ORIGINAL ARTICLE

Homogeneous reprocessing of GPS, GLONASS and SLR observations

Mathias Fritsche · Krzysztof Sośnica · Carlos Javier Rodríguez-Solano · Peter Steigenberger · Kan Wang · Reinhard Dietrich · Rolf Dach · Urs Hugentobler · Markus Rothacher

Received: 7 October 2013 / Accepted: 26 February 2014 / Published online: 25 March 2014

Abstract The International GNSS Service (IGS) provides operational products for the GPS and GLONASS constellation. Homogeneously processed time series of parameters from the IGS are only available for GPS. Reprocessed GLONASS series are provided only by individual Analysis Centers (i. e. CODE and ESA), making it difficult to fully include the GLONASS system into a rigorous GNSS analysis. In view of the increasing number of active GLONASS satellites and a steadily growing number of GPS+GLONASS-tracking stations available over the past few years, Technische Universität Dresden, Technische Universität München, Universität Bern and Eidgenössische Technische Hochschule Zürich performed a combined reprocessing of GPS and GLONASS observations. Also, SLR observations to GPS and GLONASS are included in this reprocessing effort. Here, we show only SLR results from a GNSS orbit validation. In total, 18 years of data (1994–2011) have been processed from altogether 340 GNSS and 70 SLR stations. The use of GLONASS observations in addition to GPS has no impact on the estimated linear terrestrial reference frame parameters. However, daily station positions show an RMS reduction of 0.3 mm on average for the height component when additional GLONASS observations can be used for the time series determination. Analyzing satellite orbit overlaps, the rigorous combination of GPS and GLONASS neither improves nor degrades the GPS orbit precision. For GLONASS, however, the quality of the microwave-derived GLONASS orbits improves due to the combination. These findings are confirmed using independent SLR observations for a GNSS orbit validation. In comparison to previous studies, mean SLR biases for satellites GPS-35 and GPS-36 could be reduced in magnitude from −35 and −38 mm to −12 and −13 mm, respectively. Our results show that remaining SLR biases depend on the satellite type and the use of coated or uncoated retro-reflectors. For Earth rotation parameters, the increasing number of GLONASS satellites and tracking stations over the past few years leads to differences between GPS-only and GPS+GLONASS combined solutions which are most pronounced in the pole rate estimates with maximum 0.2 mas/day in magnitude. At the same time, the difference between GLONASS-only and combined solutions decreases. Derived GNSS orbits are used to estimate combined GPS+GLONASS satellite clocks, with first results presented in this paper. Phase observation residuals from a precise point positioning are at the level of 2 mm and particularly reveal poorly modeled yaw maneuver periods.

Keywords GPS · GLONASS · SLR · Multi-GNSS processing · GNSS satellite clocks

M. Fritsche (✉)· R. Dietrich
Institut für Planetare Geodäsie, Technische Universität Dresden, Dresden, Germany
e-mail: mathias.fritsche@tu-dresden.de

C. J. Rodríguez-Solano · P. Steigenberger · U. Hugentobler
Institut für Astronomische und Physikalische Geodäsie, Technische Universität München, Munich, Germany

K. Sośnica · R. Dach
Astronomisches Institut, Universität Bern, Bern, Switzerland

K. Wang · M. Rothacher
Institut für Geodäsie und Photogrammetrie, Eidgenössische Technische Hochschule Zürich, Zurich, Switzerland

1 Introduction

Since the official start of the International GNSS Service (IGS, Dow et al. 2009) in 1994, global GPS data from the IGS-tracking network has been analyzed on a routine basis by its Analysis Centers (ACs). In 1998 the IGS started to recog-

nize available GLONASS data which led the IGS to initiate the International GLONASS Experiment (IGEX, Willis et al. 1999). Within the framework of IGEX combined GLONASS orbits were made available until July 2002. Afterwards, only a small number of stations continued to provide observation files containing GLONASS. Based on that, the IGS ACs associated with the European Space Agency (ESA) and the German Federal Agency for Cartography and Geodesy (BKG) continued to produce ephemerides for the GLONASS constellation. As a follow-on of IGEX, the International GLONASS Service Pilot Project (IGLOS-PP, Weber et al. 2005) was initiated in order to demonstrate the integration of new Global Navigation Satellite System (GNSS) constellations and their signals into the IGS activities. Since May 2003, the Center for Orbit Determination in Europe (CODE) has been providing GNSS products based on a rigorous multi-system combination of GPS and GLONASS.

Due to the growing number of GPS+GLONASS-tracking receivers in recent years, additional IGS ACs started to deliver products for both satellite systems. Starting with September 26, 2010, GLONASS ephemerides are also combined by the IGS analysis center coordinator. However, the orbit products of both GNSS are generated separately, which weakens the consistency obtainable from the rigorous inter-system contributions from the individual ACs.

Usually, changes in the processing strategies or in the realization of the reference frame cause systematic effects in both, the parameter time series of the individual ACs and in the combined IGS products. In consequence, the IGS decided to initiate a reprocessing campaign (Rebischung et al. 2012) to ensure a homogeneous input from the ACs. However, all reprocessing activities of the IGS have been limited to GPS until now. Additional observations of a steadily growing number of stations also tracking GLONASS are added to the GNSS analysis at the expense of consistency. Only individual ACs recently made available reprocessed solutions based on a combined multi-system processing scheme, e.g., CODE in 2011.

Several parameters obtained from GNSS solutions strongly depend on the antenna phase center models applied during the procedure of observation reduction. Corresponding satellite antenna models are also intrinsically linked to the underlying terrestrial reference frame (TRF). Hence, a validation of GNSS-derived parameters with independent geodetic observations is preferable in order to assess the level of consistency among the different techniques. Here, we use Satellite Laser Ranging (SLR) observations to validate our GNSS orbit products.

Starting at the level of GNSS RINEX (Receiver INdependent EXchange Format) observations and SLR normal points, a complete reprocessing was jointly carried out putting together the experience of each group at Technische Universität Dresden, Technische Universität München (both Germany), Universität Bern and Eidgenössische Technische Hochschule Zürich (both Switzerland). The overall processing comprises 18 years of GPS and SLR data from the beginning of 1994 to the end of 2011. GLONASS observations are included in the analysis starting with January 1, 2002.

This paper concentrates on the investigation of the impact of including GLONASS in a rigorous combined multi-GNSS processing scheme applying up-to-date modeling standards. In particular, we discuss results associated with the realization of a TRF, changes in the quality of the GNSS orbits, Earth rotation parameters (ERP), and GPS and GLONASS satellite clocks. Identical modeling standards are applied to SLR observations which allow a rigorous computation and an analysis of range residuals with respect to GNSS orbits.

2 Data modeling and processing strategy

We selected a set of 340 GNSS and 70 SLR stations for this reprocessing project (see Fig. 1). The primary selection criteria included a preferably long observation time span, the availability of GPS and GLONASS observations, the co-location between both space geodetic techniques GNSS and SLR and the assignment of IGS08 reference frame stations (Rebischung et al. 2012). GLONASS-only tracking sites, sporadically available in the late 1990s, have not been taken into account. For the clock solution we selected a reduced set of overall 320 GNSS stations whose type of operating clock and global distribution are of best possible quality.

The reprocessing starts on January 1, 1994, with a GPS-only network of about 40 stations and continues till the end of 2011. Due to the sparse number of sites providing observations from both GNSS, GLONASS observations are not included in the processing before January 1,

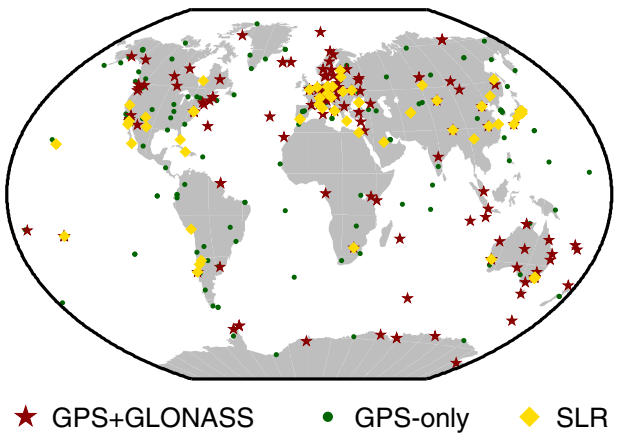

Fig. 1 Geographical distribution of GPS+GLONASS receivers (*red stars*), GPS-only receivers (*green dots*) and SLR stations (*yellow diamonds*) used for the reprocessing

2002. GPS+GLONASS receivers are operated at 135 out of the total of 340 sites at least for a couple of weeks. However, due to continuous changes in the station network and site-specific hardware configuration the total number of stations per day does not exceed 254. The maximum number of 106 GPS+GLONASS-tracking receivers is reached only at the end of 2011 (see Fig. 2, top). Consequently, only 40 % of the stations support GLONASS at the maximum which makes GPS dominating the solution. For SLR, the number is nearly constant with 17 observing stations on a weekly average.

2.1 Data modeling

We use a modified version of the Bernese GNSS Software Version 5.1 (Dach et al. 2007) to process microwave measurements from GPS and GLONASS as well as the SLR range measurements. Zero-difference code observations are used for the estimation of GNSS clocks and differential code biases. Zero-difference phase observations serve for the generation of combined code+phase and phase-only clock solutions. All remaining parameter estimates are derived from a least-squares adjustment of phase observations (double-differences) or laser range measurements.

Steigenberger et al. (2006) provide a comprehensive description of the basic GNSS data modeling which, in principle, also applies for this reprocessing. Accordingly, Table 1 addresses only major differences which are mainly due to updated standards. In particular, we make use of site positions (IGS08) and GNSS-specific absolute corrections for antenna phase center offsets (PCOs) and phase center variations (PCVs) for receivers and satellites (Dach et al. 2011) that all are associated with the realization of the latest International Terrestrial Reference Frame ITRF2008 (Altamimi et al. 2011). If no GLONASS-specific receiver antenna PCVs are available the corresponding values from GPS are adopted. For the troposphere we apply a priori ECMWF-based hydrostatic delays involving the dry VMF1 mapping function (Böhm et al. 2006), while the wet VMF1 is used for the zenith delay parameter estimation.

Usually, the effect of direct solar radiation pressure is taken into account for GNSS satellite orbit modeling by applying physical (e.g., Fliegel et al. 1992; Fliegel and Gallini 1996) or empirical (e.g., Springer et al. 1999) models. However, due to the absence of a consistent set of radiation pressure coefficients for all types of satellites (see Fig. 2, bottom) no a priori solar radiation pressure is taken here into account. Rather, we estimate five radiation pressure parameters per satellite (cf. Beutler et al. 1994 model) in addition to the six orbital elements which ensures a clean environment for the determination of a consistent empirical model. In addition, we introduce the acceleration due to Earth radiation pressure and antenna thrust (Rodríguez-Solano et al. 2012a) on the computation of GNSS satellite orbits (Table 1). The antenna thrust acceleration is only applied for GPS satellites, because no information about the navigation antenna power of GLONASS satellites is available so far.

Solid Earth tides are modeled according to the IERS Conventions 2003 (McCarthy and Petit 2004). Site displacements due to ocean tidal loading are derived from the EOT11a model (Savcenko and Bosch 2012). For site displacements due to atmospheric pressure tidal loading, the Ray and Ponte (2003) model is applied to account for the $S_1 + S_2$ tidal effect. Associated non-tidal load displacements are derived from the Gravity Recovery and Climate Experiment (GRACE) AOD1B atmospheric and ocean dealiasing product (Flechtner 2007). Tidal and non-tidal contributions are handled consistently, because the Ray and Ponte (2003) model is also used for the generation of the AOD1B products. The corresponding spherical harmonic coefficients are given at a 6-h sampling and are also available for the time period previous to the GRACE satellite mission. Using the coefficients from 1994 to 2009 a linear model is derived and applied for detrending the input time series. In addition, each set of coefficients is supplemented with a load potential that is in hydrostatic equilibrium with the total load's gravitational potential field (cf. Clarke et al. 2005; Fritsche et al. 2012). We derive load-induced site displacements applying a global convolution with load

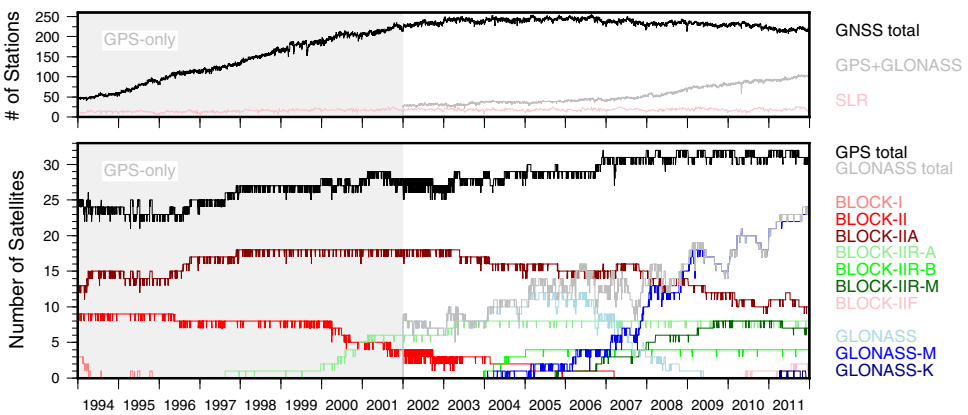

Fig. 2 Number of reprocessed stations and satellites. Starting with January 1, 2002, GLONASS is included in the processing. *Top* total number of GNSS-tracking receivers (*black*), number of receivers tracking GPS+GLONASS (*grey*) and total number of SLR stations (*pink*). *Bottom* total number of GPS (*black*), GLONASS (*grey*) and block-specific satellites

Table 1 Summary of observation modeling and parameter estimation strategy

GNSS and SLR		
Radiation pressure	Direct:	No a priori model applied for GNSS, cannonball model for LAGEOS
(orbit modeling)	Earth radiation:	Visible and infrared for GPS and GLONASS,
	(albedo)	antenna thrust for GPS only (Rodríguez-Solano et al. 2012a),
		numerical Earth radiation pressure model from monthly averaged
		reflectivity and emissivity coefficients (http://www.iapg.bv.tum.de/albedo)
	Empirical	D0: constant (direction of the Sun)
	Parameters	Y0: constant Y-bias (direction along the solar panel axis)
	(accelerations):	B0, B-cos, B-sin: constant and once per revolution
Gravity potential	EGM 2008 max. degree/order: 30 (Pavlis et al. 2012)	
Ocean tide model	CSR 3.0 max. degree/order: 8 (Eanes and Bettadpur 1996)	
Solid earth tides	IERS 2003 conventions (McCarthy and Petit 2004)	
Ocean loading	Tidal:	Multi-mission altimetry model EOT11a (ftp://ftp.dgfi.badw.de/pub/EOT11a),
		Corrections computed by the free ocean tide loading provider
		(http://holt.oso.chalmers.se/loading/index.html)
	Non-tidal:	6-hourly GRACE AOD1B atmospheric and ocean de-aliasing product
Atmospheric pressure	Tidal:	$S_1 + S_2$ corrections from Ray and Ponte (2003) model
Loading displacements	Non-tidal:	6-hourly GRACE AOD1B atmospheric and ocean de-aliasing product
		(http://isdc.gfz-potsdam.de)
Earth orientation	A priori polar motion and UT1–UTC from IERS C04 series aligned to ITRF2008	
GNSS-only		
Troposphere	Zenith delay:	6-hourly ECMWF-based hydrostatic delay mapped with VMF1
A priori		(Böhm et al. 2006, http://ggosatm.hg.tuwien.ac.at/DELAY)
	Gradients:	Not applied
Troposphere	Zenith delay:	2-hourly station-wise mapped with wet VMF1 mapping function
Estimation	Gradients:	24-hourly station-wise mapped with the Chen and Herring (1997)
		gradient mapping function
Ionosphere	Elimination of first-order term by forming ionosphere-free linear combination	
	Modeling of second- and third-order terms, and ray bending effect	
Terrestrial reference	ITRF2008 realized through station coordinates and velocities given in IGS08 (Rebischung et al. 2012)	
Frame	Datum	No-net translation conditions
	Definition:	No-net rotation conditions
Antenna phase center	`IGS08_1633.atx` (http://igs.org/igscb/station/general)	
SLR-only		
Troposphere	Zenith delay:	Mendes and Pavlis (2004) model for zenith path delay and mapping function,
A priori		corrections estimated on the basis of site-specific meteorological data
Laser retro-reflector	Array offsets according to the recommendations of the ILRS (Pearlman et al. 2002)	
Terrestrial reference frame	ITRF2008 realized through a set of station coordinates and velocities given in SLRF2008	

Note, some of the processing standards differ from those recommended for the second IGS reprocessing campaign (http://acc.igs.org/reprocess2.html)

Love numbers in the center of mass frame (CM, Blewitt 2003).

Within this reprocessing project, SLR range measurements to GPS and GLONASS satellites are processed. At optical wavelengths, the tropospheric delay is described by the Mendes and Pavlis (2004) model with the associated mapping function of submillimeter accuracy for elevation angles above 10°. Station coordinates are represented in the SLRF2008 (Pavlis 2009). Using the same processing software, we can assure consistency among all model components that microwave and optical measurement techniques have in common. In particular, the application of a fully consistent orbit model for the GNSS satellites, the same reference frame, and identical procedures to correct for tidal and non-tidal site displacements as well as for other processing components (e.g., relativistic corrections) are guaranteed.

2.2 Processing strategy

The multi-system reprocessing scheme for GNSS is adapted from that used operationally at the CODE IGS AC (Dach et al. 2009). The processing starts at the level of RINEX observation data. Before January 1, 2002, we use results from the first IGS reprocessing campaign to derive a priori GPS ephemerides. For GLONASS ephemerides, we merge navigation messages and products from ACs that participate in the IGEX. For Earth rotation, we introduce the IERS C04 ERP series (Bizouard and Gambis 2009) aligned to ITRF2008 as a priori information. For the data preprocessing a priori global ionosphere maps and differential code biases resulting from a first reprocessing run (1994–2009, Steigenberger et al. 2006) and operational CODE product series (2010–2011) were introduced. Starting with January 1, 2002, observations from GLONASS are rigorously combined with that from GPS in all processing steps. However, double-difference ambiguities are solved only for GPS according to the strategy described in Steigenberger et al. (2006). A sophisticated algorithm to verify the resolved ambiguities (Dach et al. 2011) was added.

We compute 1-day ambiguity-fixed GPS-only solutions for the entire time span. Starting with January 1, 2002, we additionally compute a second solution from the simultaneous adjustment of GPS+GLONASS observations with only the GPS ambiguities fixed and a third GLONASS-only solution. The associated normal equation (NEQ) systems include station coordinates, site-specific troposphere parameters (zenith delays, gradients), satellite orbit parameters (Keplerian elements, dynamic and pseudo-stochastic parameters), Earth orientation parameters (polar motion, UT1–UTC), and three scaling factors per site (one for each topocentric component) with respect to the a priori atmospheric pressure loading model. The scaling factors may serve for validation purposes. However, all solutions discussed here are generated with the non-tidal pressure loading corrections included by forcing the scaling factors to unity.

To strengthen the GNSS satellite arc stability, our orbits are derived from 3-day solutions which are created by stacking corresponding daily parameters. In preparation for this NEQ stacking, we first generate daily station position time series for the entire data period which are analyzed using the Bernese GNSS Software tool FODITS (Ostini 2012). In the event of significant discontinuities, we estimate multiple station coordinate sets in the 3-day combination and pre-eliminate daily coordinate parameters marked as outliers. Continuous piece-wise linear ERPs, initially set up at 1-h intervals, are transformed to daily parameters with the first UT1–UTC parameter of a satellite arc fixed to the a priori value. Each 3-day arc is represented by one set of osculating elements, one set of radiation pressure parameters and pseudo-stochastic pulses at 12-h intervals. In case of modeling problems or maneuvers, we split up the 3-day arc into two or even three segments. In general, arc splitting is suppressed for a particular satellite if its number of observations for a day involved is less than 50 % of the average from all the satellites of the same system. Likewise, no pulses are estimated if the satellite's observation count is less than 15 % of the averaged observation number for GPS and 25 % for GLONASS. For stations defining the geodetic datum the resulting coordinates are compared to their a priori IGS08 values using a seven-parameter similarity transformation. Stations with residuals larger than 10 mm for the horizontal or 30 mm for the height component are excluded from the datum definition which is imposed by no-net translation and no-net rotation conditions.

The zero-difference observation processing for the computation of receiver and GPS+GLONASS satellite clock corrections is performed in a separate run. Estimated satellite orbits, ERPs, station coordinates and troposphere parameters from the 3-day solution are introduced as fixed values. The station selection made for the clock computation differs from that used in the double-difference processing. Nevertheless, our approach ensures consistency among all estimated parameters. The clock processing includes the 24-h midnight epoch which allows us to align consecutive daily clock solutions with each other. The analysis procedure involves the pre-processing of zero-difference code observations, the computation of inter-system and inter-frequency code biases, and the pre-processing of zero-difference phase observations. Based on the ionosphere-free linear combination, we estimate 5-min station and satellite clock offset parameters. Introducing the 5-min clock results, 30-s satellite clock corrections are obtained from an interpolation based on phase observations (Bock et al. 2009). Two types of solutions are available: (1) a combination of code and phase measurements and (2) using only phase measurements.

In this study, laser range measurements to GPS and GLONASS satellites are processed only for orbit validation purposes, but do not contribute to the global solution. We introduce the satellite orbits and ERP estimates from our final 1- and 3-day solution as fixed values. No range biases are estimated. The SLR measurements to GNSS satellites refer to the Laser Retro-reflector Array (LRA), whereas the associated orbit parameters refer to the satellite's center of mass. Accordingly, we apply the LRA offsets provided by the International Laser Ranging Service (ILRS, Pearlman et al. 2002) for the computation of the laser range residuals to GNSS satellites.

3 Results

One of the study's key objective concerns the impact of combining GPS and GLONASS on different parameter types and products derived therefrom. Hence, we focus our analysis on parameter time series derived from the simultaneous processing of both GNSS.

3.1 Terrestrial reference frame

We accumulate consecutive 1-day NEQ systems and combine station coordinates and velocities, and continuous piecewise linear daily ERPs. Based on the outlier information used to generate the 3-day solutions, corresponding 1-day coordinate parameters are pre-eliminated and position discontinuities are introduced, each of which leads to a new set of coordinates and velocities. Pole coordinates and length of day parameters are freely estimated. UT1–UTC parameters are fixed to the a priori IERS C04 series. To obtain a minimum-constraints solution, we add no-net rotation conditions for the network orientation and the orientation rate using a priori IGS08 values for fiducial sites. If a discontinuity refers to an event other than an earthquake we do not allow for a relative velocity change by introducing additional constraints (cf. Rülke et al. 2008).

Applying the procedure described above to appropriate NEQ systems from 2002 to 2011, we derive coordinate and velocity estimates for 324 sites for both, a GPS-only and a GPS+GLONASS combined solution. In total, 135 of these sites provide observations from GLONASS satellites. However, the relative number of GLONASS with respect to GPS observations is clearly uneven over time. At the beginning of 2002 the relative contribution of GLONASS to the combined solution is only 2 % and does not exceed 6 % until the end of 2007. Afterwards, it steadily increases to almost 25 % at the end of 2011. This also becomes obvious if we compare the system-specific number of observation days for the GPS+GLONASS-tracking sites shown in Fig. 3. Whereas more than 50 % of those sites observe GPS for 9–10 years, there are only 10 % providing GLONASS for such a long period. Rather, the majority of sites contributes only up to 5 years of GLONASS data. In addition, the GLONASS contribution has a generally lower impact on the coordinate results, because ambiguities have only been resolved for GPS.

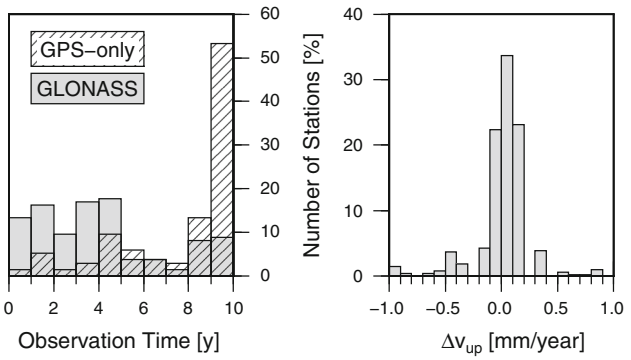

Fig. 3 Contribution of GLONASS to a combined GNSS processing (2002–2011, 135 GPS+GLONASS sites). *Left* comparison of system-specific observation time. *Right* differences in vertical station velocities computed from a GPS-only and a GPS+GLONASS terrestrial reference frame solution

To evaluate the GLONASS contribution to the determination of a TRF, we first compare our coordinate and velocity estimates to IGS08 applying a 14-parameter similarity transformation with the reference epoch at January 1, 2007. The same set of sites defining the geodetic datum is used in all transformations. Table 2 provides a summary of the parameter estimates which reveal similar values for the combined and the GPS-only solution. For GPS-only the translation offset estimates are −4.3, −7.0, −2.8 mm for the X-, Y-, and Z-component, respectively. This order of magnitude shows a good agreement with the results of Rülke et al. (2008) who also determined a GPS-only TRF. Likewise, our translation offsets show the discrepancy in the realization of CM from GNSS and, due to the alignment of IGS08 to ITRF2008, from SLR. The absolute values of associated rate estimates are not larger than 1.3 mm/year. The IGS08 scale and scale rate are intrinsically linked to the input data from SLR and Very Long Baseline Interferometry to ITRF2008. Mean network scale differences are not larger than −2.7 mm (−0.4 ppb) when related to the Earth's radius, but are directly affected by imperfect observation reduction models. More importantly, absolute scale rate estimates do not exceed 0.1 mm/year (0.02 ppb/year) which confirms a consistent scale realization over time. The rotational components are zero due to the imposed datum definition. In addition to the TRF transformations, we compute the differences in vertical motion between the GPS-only and the combined GNSS solution for all sites involved. Figure 3 shows a histogram of the differences which are below 0.2 mm/year for most of the sites.

For both types of solutions, we derive site position time series from a comparison of daily coordinate estimates with respect to the corresponding TRF. Applying a time-correlated noise model (white plus flicker noise), harmonic coefficients for annual, semi-annual and draconitic periods are estimated. The length of the time series does not suffice to separate the GPS (351.5 days) and GLONASS (353.2 days) specific draconitic year. Hence, we adopt a mean period of 352.3 days. The root mean square (RMS) of the time series adjustment is taken as a measure of the station position repeatability. To account for short data periods, we require a minimum observation interval of 6 years which leaves 231 stations for the analysis. Power on the annual frequency is most probable due to unmodeled loading phenomena, e.g., continental water storage (Dam et al. 2001). Contributions from the draconitic period are also evident and are related to orbit mismodeling or multipath (Ray et al. 2008; Rodríguez-Solano et al. 2012; Amiri-Simkooei 2013). Figure 4 shows changes in amplitude of the annual and draconitic fraction and in the RMS if we include GLONASS into the processing. Changes in amplitudes are largest for the vertical component, but rarely exceed 0.25 mm with no distinct increase or decrease in magnitude.

Table 2 Terrestrial reference frame comparisons

IGS08 with respect to	Translations (mm)/ translation rates (mm/year)			Scale (mm)/ scale rate (mm/year)
	X	*Y*	*Z*	
GPS+GLONASS	-4.0 ± 0.1	-6.7 ± 0.1	-2.6 ± 0.1	-2.7 ± 0.2
	-1.0 ± 0.0	$+1.2 \pm 0.0$	$+0.7 \pm 0.0$	-0.1 ± 0.0
GPS-only	-4.3 ± 0.1	-7.0 ± 0.1	-2.8 ± 0.1	-2.6 ± 0.2
	-1.1 ± 0.0	$+1.3 \pm 0.0$	$+0.7 \pm 0.0$	-0.1 ± 0.0

Results of a 14-parameter similarity transformation of IGS08 with respect to GPS+GLONASS combined and GPS-only TRFs. Rotation parameters are defined to be zero and, hence, not shown here. Reference epoch for offset parameters is 01 January, 2007. Scale parameters refer to the Earth's radius

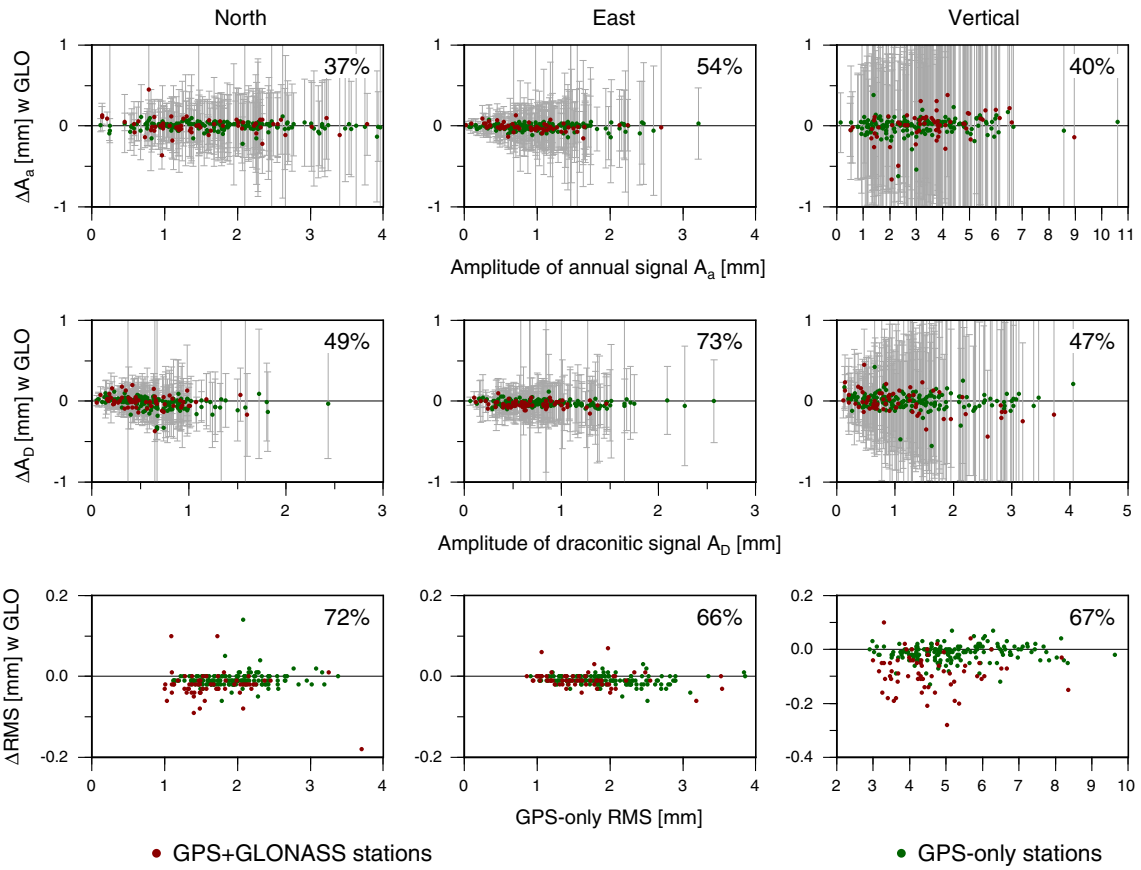

Fig. 4 Time series analysis of daily GNSS station positions. Amplitudes of the annual period (*top*) and draconitic year (*center*), and root mean square (RMS, *bottom*) estimated from the GPS-only solution and corresponding changes due to including GLONASS in the processing. Negative values mean a reduction of the RMS in time series from the GPS+GLONASS combination. Values in percentage indicate the number of sites showing a reduction. *Grey bars* give uncertainty of the amplitude differences

In terms of their error estimates, resulting amplitude differences are not significant. The induced RMS difference is small in magnitude not exceeding 0.1 mm for the horizontal and 0.3 mm for the vertical component. However, the majority of sites show an RMS reduction while the largest effect can be identified for those sites which additionally observe GLONASS (red dots in Fig. 4).

3.2 GNSS orbits

In order to evaluate the impact of combining GPS and GLONASS on the estimated satellite orbit quality, we compute median overlaps of 1- and 3-day satellite arcs. For the latter, overlaps are the position differences at the end of the middle day of a 3-day arc and the beginning of

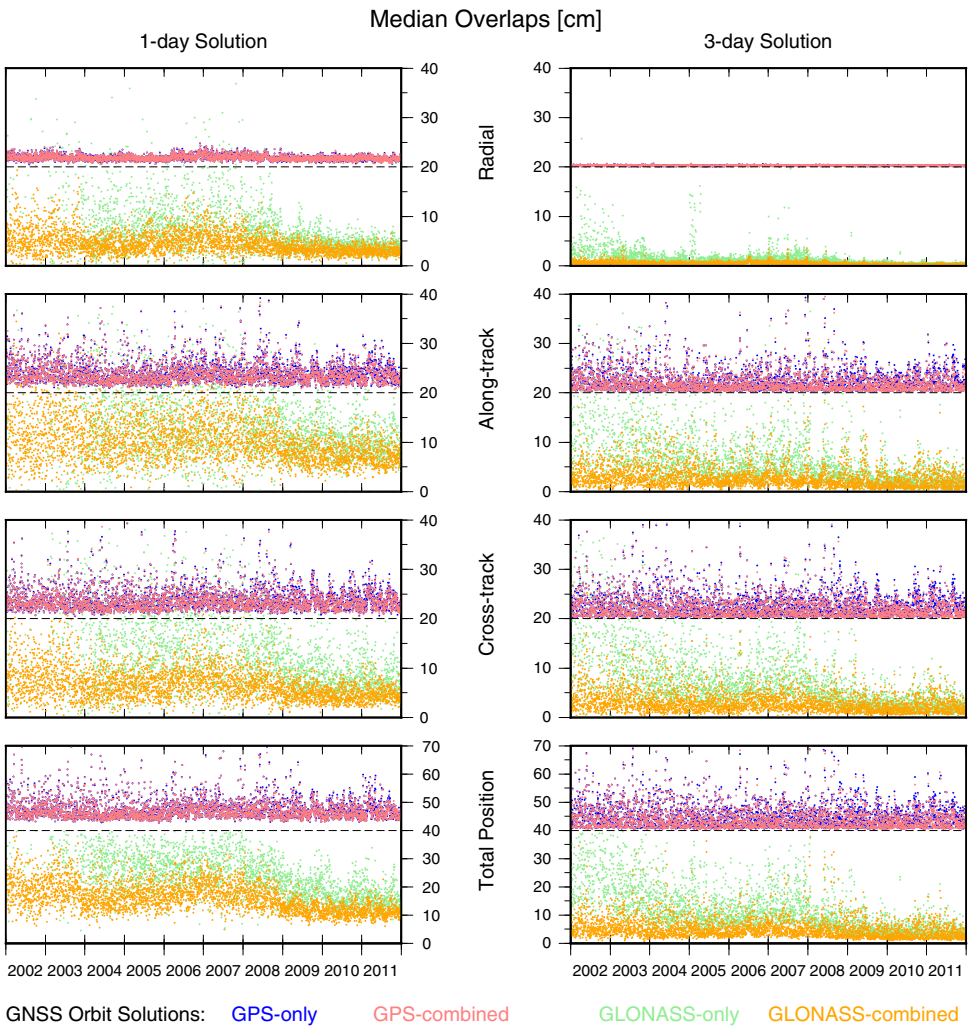

Fig. 5 Median overlaps for daily satellite arcs derived from 1-day (*left*) and 3-day (*right*) solutions. GPS satellites from GPS-only (*blue*) and GPS+GLONASS combined (*pink*) solutions (shift: +20, +40 cm for total position). GLONASS satellites from GLONASS-only (*green*) and GPS+GLONASS combined (*yellow*) solutions. Eclipsing satellites and satellites with large overlaps are excluded

the middle day of the next 3-day arc. Figure 5 shows the results for GPS and GLONASS satellites based on the GPS-only, GLONASS-only and GPS+GLONASS combined solutions. The overlaps are computed in radial, along- and cross-track directions and are also provided for the total position difference. Eclipsing satellites and satellites with overlaps larger than 0.4 m (mostly the case in the early GLONASS years) are excluded from the statistics.

For GPS satellite arcs derived from individual 1-day solutions, we see that the total position differences amount to about 4–20 cm (Fig. 5, bottom left) with the largest contribution from the along-track components. Looking at the individual components, no significant improvement can be observed when combining GPS and GLONASS. For GLONASS satellites, the total position differences from the GLONASS-only solutions are at a level of about 30 cm (Fig. 5, bottom left) and continuously decrease as the number of GLONASS satellites and tracking stations increases. For the combined solution, corresponding overlaps are significantly reduced to about 10–20 cm. Hence, the combination with GPS improves the quality of the estimated GLONASS satellite orbits by about 50 %.

We use the long-arc solution in order to stabilize the GLONASS orbits. In consequence, the overlaps referring to the middle day of the 3-day satellite arcs are smoothed and the daily solutions are not independent anymore. For the total position difference the lower bound of the median is reduced to about 1–2 cm for GPS satellites in both, the GPS-only and combined solutions (Fig. 5, bottom right). Again, no significant impact from the combination can be deduced for GPS satellites. The reduction in the median overlap magnitude is substantial for GLONASS. As for the 1-day arcs, the GLONASS-only results reveal a strong time-dependence related to the number of satellites and tracking stations. The corresponding median for the total position difference varies in a range between about 25 cm in 2002 and 3 cm at the end of 2011. Combining GPS and GLONASS, the quality of the GLONASS orbits can be improved until the end of 2007. Starting with 2008, almost no difference is evident due to the combination. This leads to the conclusion that a global

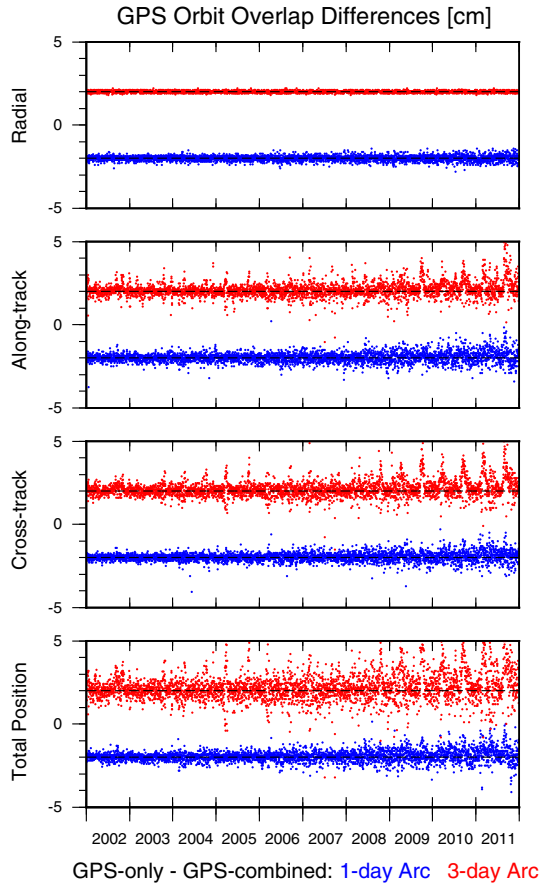

Fig. 6 Differences between the median GPS orbit overlaps from the GPS-only and the GPS+GLONASS combined solutions. Differences are computed for 1-day (*blue*, shift: −2 cm) and 3-day (*red*, shift: +2 cm) arc solutions

GLONASS-tracking network has been established approximately by this time. In the latest years, the magnitude of the overlaps is very similar to that of GPS for all components.

To test the impact of the combination on the estimated GPS orbits, we also compute the difference between the obtained GPS-only and GPS+GLONASS-based overlaps. Figure 6 shows the overlap differences derived from 1-day and 3-day arcs. In general, the continuous increase in the number of GLONASS satellites and GLONASS-tracking stations leads to increased differences for the latest years which is most pronounced in along- and cross-track directions. Semi-annual patterns are clearly evident and might be related to orbit modeling deficiencies. For the total position differences, the scatter is generally larger when derived from 3-day arcs. Our findings indicate that including GLONASS has a larger impact on estimated GPS satellite positions when processing longer satellite arcs. In addition, the impact shows a periodic behavior indicating problems with satellite orbit modeling.

To assess the external orbit quality, we compare our 3-day orbits with other solutions by means of a seven-parameter similarity transformation of three-dimensional satellite positions. Figure 7 (top) shows the results for the RMS. Our findings show that the agreement is at the level of 1–3 cm when compared to IGS GPS satellite positions from the first reprocessing campaign and operational products. An increase in RMS can be observed with respect to the IGS reprocessed orbits starting on March 12, 2006 (GPS week 1366). The reason for that remains unknown. However, it might be worth noting that the discontinuity epoch coincides with the start of a new GPS week and that afterwards the scatter is similar to that of the operational IGS orbits. Moreover, we make use of the CODE reprocessing series[1] that also rigorously combines GPS and GLONASS but uses different modeling options. Here, the RMS for GPS is at the same level as that for IGS but does not show an increase in 2006. For GLONASS, the RMS varies between 3 and 5 cm on average.

3.3 GNSS orbit validation using SLR

The SLR observation technique provides a precise and independent way to validate and assess the quality of GNSS orbits. As opposed to microwave measurements, its particular strength originates from the absolute range information, which is disturbed by only few error sources (Thaller et al. 2014). However, laser ranging to GNSS satellites is very demanding due to the high orbit altitude, and thus, low energy of a return pulse. Predominantly, SLR-based residuals are an indicator for the radial accuracy of the microwave-derived orbits, because the maximum angle of incidence of the laser pulse to a satellite is only about 13° and 14° for GPS and GLONASS satellites, respectively.

Unfortunately, only two GPS satellites are equipped with an LRA, namely GPS-35 (launch date 30 August, 1993) and GPS-36 (launch date 10 March, 1994). GPS-36 was continuously observed by the ILRS network between 1994 and 2011, whereas observations of GPS-35 were continuous until its decommission in 2009. With regard to GLONASS, all satellites are equipped with a LRA. Despite the ILRS recommendations, several SLR stations track the full GLONASS constellation. In total about 91,000 SLR normal point observations to GPS and 229,000 to GLONASS are processed (Table 3).

In a first step, we analyze residuals derived with respect to the GPS+GLONASS combined 3-day orbit solutions. Mean biases of the residuals and associated RMS values are summarized in Table 3. In comparison to earlier studies we notice a crucial improvement. That is, the biases of −35 mm for GPS-35 and −38 mm for GPS-36 reported by Flohrer (2008) are reduced to −12 and −13 mm, respectively. Associated RMS values of 22 and 27 mm could be reduced to 21 mm.

[1] ftp://ftp.unibe.ch/aiub/REPRO_2011/CODE

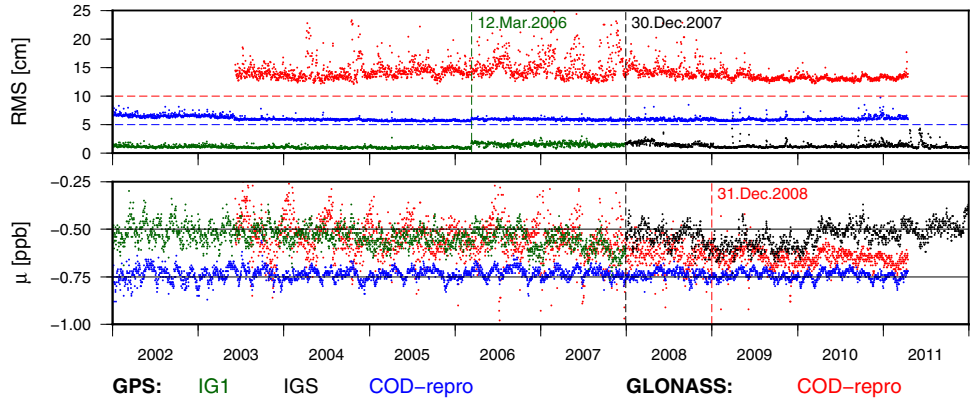

Fig. 7 Comparison of final three-dimensional satellite positions. Root mean square (RMS, *top*) and scale difference (*bottom*) of a seven-parameter similarity transformation. GPS satellite positions are compared to IGS repro-1 (*IG1*), IGS operational (*IGS*) and CODE reprocessing (*COD-repro*) products. GLONASS satellite positions are compared to the CODE reprocessing products. RMS values of COD-repro are shifted by 5 and 10 cm, respectively

The improvements are due to taking into account Earth radiation pressure and antenna thrust, a consistent reference frame scale, common loading effects and an improved troposphere model. Including atmospheric loading corrections for SLR in our study reduces the so-called Blue-Sky effect (Sośnica et al. 2013).

The mean bias for the overall GLONASS constellation is −3 mm with an RMS of 34 mm for the range residuals. For comparison, Flohrer (2008) reports biases between −10 and +5 mm with RMS values ranging between 46 and 57 mm (Table 3). The biases do not seem to be plane-dependent. Rather, they are related to the satellite type which is supported by an RMS reduction from 38 mm for early GLONASS type satellites to 32 mm for the GLONASS-K satellite. Here, results reported for the GLONASS-K satellite have to be considered with care because it was active for microwave-tracking only for a very short time interval (see Fig. 2). The mean bias referring to all GLONASS-M type satellites (−3.1 mm) compares well to that of early GLONASS type satellites (−2.7 mm). However, GLONASS-M type satellites launched before 2010 are usually equipped with a coated LRA, whereas most of them launched in 2010–2011 (e.g., R09, R12, R16, R17) are equipped with uncoated LRAs (asterisk in Table 3). Also, newer launched satellites have a different number of retro-reflectors in the reflector array. If we consider only GLONASS-M type satellites with a coated LRA, we obtain a mean bias of −0.8 mm. For GLONASS-M type satellites without coating, the mean bias is −7.6 mm which compares better to that for the GLONASS-K type (−6.6 mm). Using the scatter of the satellite-specific biases to compute the standard deviation of the mean bias for each satellite type, we obtain 19.0 mm for the early GLONASS type, 8.5 mm for the coated and 11.5 mm for the uncoated GLONASS-M type (no value is computed from the only GLONASS-K type satellite). Thus, differences between satellite-type mean biases are not significant in a statistical sense. Nevertheless, the use of uncoated LRAs for newly launched GLONASS satellites possibly leads to larger biases similar to GPS (Thaller et al. 2012).

Following Urschl et al. (2007), we analyze the residuals in a system defined by the satellite orbit angle Δu (argument of satellite latitude with respect to argument of latitude of the Sun) and the Sun's elevation β_0 above the orbital plane. Looking at Fig. 8, variations of the bias are visible for GPS-36. The bias reaches −20 mm if Δu is between 120° and 240° (night-time tracking) and is close to 0 mm otherwise (day-time tracking). GLONASS satellites reveal also systematic residual patterns which can be associated with orbit modeling deficiencies. For R22, Fig. 8 shows mean residuals of approximately +60 mm in maximum when the Sun is inclined by $\beta_0 = \pm 20°$ and Δu is about 180°. We observe negative mean residuals of about −80 mm in minimum when Δu is close to 0°.

In addition to the GPS+GLONASS combined 3-day orbits, we analyze the residuals derived with respect to the remaining single system 3-day and all three 1-day orbit solutions. Figure 9 shows mean biases and associated RMS values computed separately for GPS BLOCK-IIA, GLONASS, GLONASS-M (coated and uncoated) and GLONASS-K type satellites. For GPS satellites, the comparison between GPS-only and GPS+GLONASS combined solutions shows very small differences. With GLONASS included, the RMS values for 3-day arcs increase by 0.3 mm while the mean biases are reduced by 0.4 mm in magnitude. Generating 1-day instead of 3-day satellite arcs reveals mean biases increased by 0.3 mm in magnitude. Corresponding RMS values become larger by about 6 mm on average. Hence,

Table 3 GNSS orbit validation utilizing residuals of Satellite Laser Ranging (SLR) observations

Satellite type / *Satellite System*	COSPAR ID	SLR observation period	Orbital plane	Number of observations	This study		Flohrer (2008)	
					Mean bias (mm)	RMS of residuals (mm)	Mean bias (mm)	RMS of residuals (mm)
GPS-35 BLOCK-IIA	1993-054A	1994–2011	2	42,833	−11.5	20.2	−35	22
GPS-36 BLOCK-IIA	1994-016A	1994–2011	3	48,418	−12.9	21.6	−38	27
R01 GLONASS	1998-077A	2002	1	1,116	−8.4	38.1		
R02 GLONASS-M*	2011-065A	2011	1	1,180	−15.0	28.2		
R03 GLONASS	2001-053B	2002–2007	1	38,172	−3.5	39.1	−10	49
R03 GLONASS-M*	2011-064A	2011	1	1,367	−11.2	28.6		
R05 GLONASS-M	2009-070C	2011	1	6,596	+2.4	33.4		
R06 GLONASS	2001-053C	2002	1	4,505	+5.7	37.8		
R06 GLONASS-M	2009-070B	2011	1	940	0.0	28.0		
R07 GLONASS-M	2004-053B	2005–2008	1	21,648	+3.1	37.8	+5	57
R07 GLONASS-M*	2011-064B	2011	1	886	+4.9	29.9		
R08 GLONASS-M*	2008-067B	2009–2011	1	27,517	−18.7	30.8		
R09 GLONASS-M*	2010-041C	2011	2	1,324	−4.5	33.3		
R10 GLONASS-M	2006-062B	2011	2	1,038	−0.1	37.2		
R11 GLONASS-M	2007-065C	2008–2011	2	17,512	−8.3	37.0		
R12 GLONASS-M*	2010-041B	2011	2	1,687	−8.3	32.0		
R13 GLONASS-M	2007-065A	2011	2	1,349	−5.9	27.3		
R15 GLONASS-M	2006-062A	2007–2011	2	34,870	+7.0	37.1		
R16 GLONASS-M*	2010-041A	2011	2	1,361	−7.9	32.5		
R17 GLONASS-M*	2011-071A	2011	3	832	+0.2	45.4		
R18 GLONASS-M	2008-046A	2009–2011	3	7,843	−0.5	32.9		
R19 GLONASS-M	2007-052A	2011	3	1,229	−2.0	26.2		
R20 GLONASS-M	2007-052B	2011	3	1,247	+6.8	36.5		
R21 GLONASS-M	2008-046B	2011	3	852	+0.7	25.6		
R22 GLONASS	2002-060A	2003–2007	3	31,606	−4.5	37.2	−4	46
R22 GLONASS-M	2010-007A	2010–2011	3	1,117	−8.0	27.3		
R23 GLONASS-M	2010-007C	2010–2011	3	9,161	−1.1	36.8		
R24 GLONASS-M	2005-050B	2007–2009	3	9,218	−5.9	42.9	−3	51
R24 GLONASS-M	2010-007B	2011	3	809	+0.1	30.3		
R26 GLONASS-K	2011-009A	2011	3	2,642	−6.6	32.2		
GLONASS			1, 2, 3	229,624	−3.2	33.6		
GPS			2, 3	91,251	−12.2	20.9		
GLONASS			1	103,927	−4.1	33.2		
GLONASS			2	59,141	−4.0	33.8		
GLONASS			3	66,556	−1.9	33.9		
GLONASS			1, 3	75,399	−2.7	38.1		
GLONASS-M + GLONASS-M*			1, 2, 3	151,583	−3.1	32.9		
GLONASS-K (one satellite only)			3	2,642	−6.6	32.2		
GLONASS-M			1, 2, 3	115,429	−0.8	33.1		
GLONASS-M*			1, 2, 3	36,154	−7.6	32.6		

Microwave-based satellite orbits are the 3-day arc solutions from the combination of GPS and GLONASS. * GLONASS-M type satellites equipped with uncoated retro-reflectors

using 3-day arcs seems to be more beneficial for GPS satellites than the combination with GLONASS. For GLONASS satellites, we find that the combination with GPS strongly improves the solution for old GLONASS type satellites. Here, including GPS induces the largest relative changes in the mean bias. GLONASS-M type satellites show very

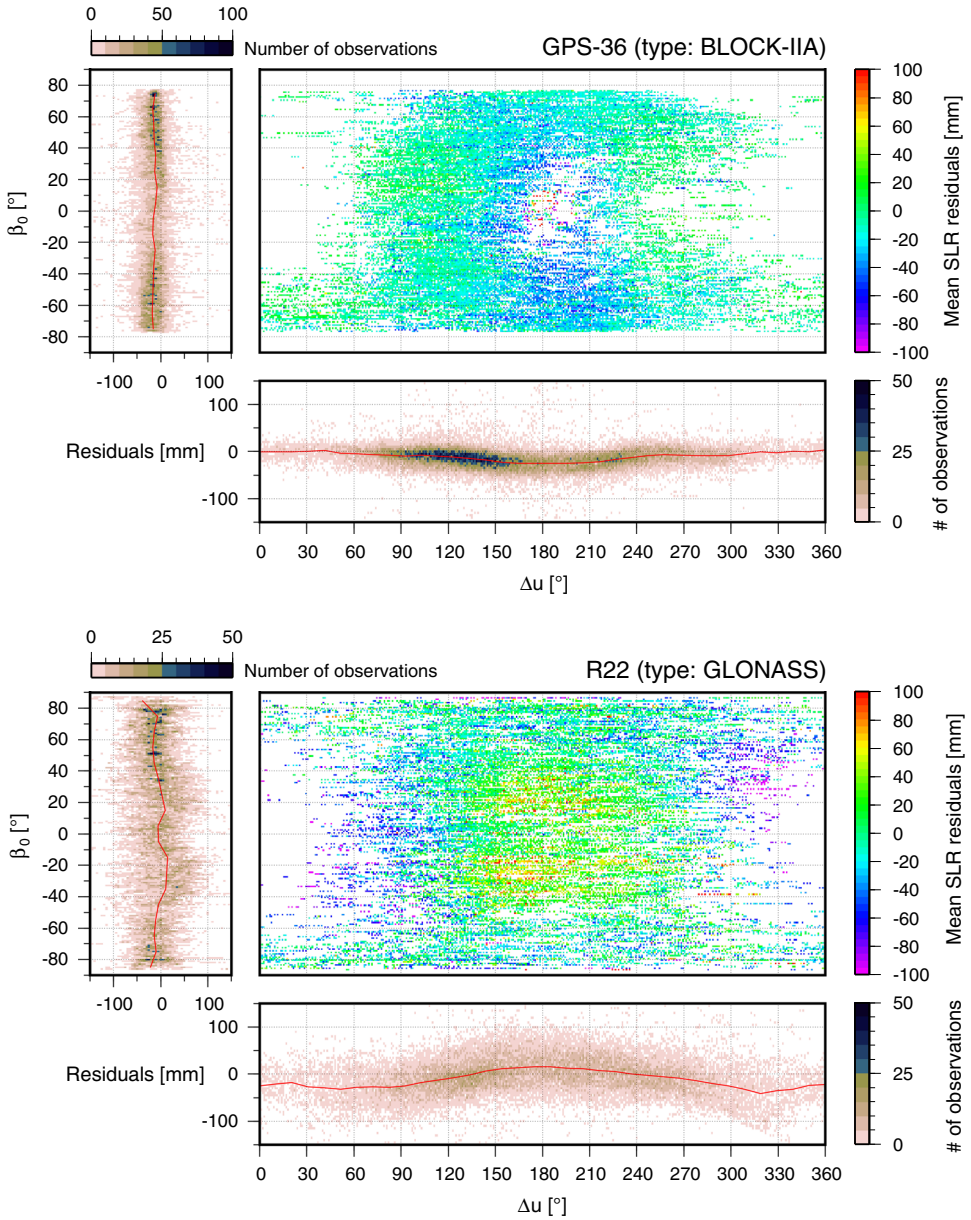

Fig. 8 Validation of microwave-based GNSS orbits for satellites GPS-36 (*top*) and GLONASS R22 (*bottom*) using satellite laser ranging (*SLR*). *Center plots* show SLR residuals (observed minus computed) projected with respect to the satellite orbit angle Δu (argument of satellite latitude with respect to argument of latitude of the Sun) and the Sun's elevation β_0 above the orbital plane. *Plots* below and to the left show the residuals (scale), number of SLR normal point observations (*color bar*), and mean biases (*red line*) depending on Δu and β_0, respectively. *Plotted* residuals cover the time span 2000–2011 for GPS-36 and 2003–2007 for R22

homogeneous results. There is almost no change in the bias neither due to including additional GPS observations nor due to processing arcs from 3-day solutions. Choosing 3-day over 1-day arcs improves the RMS only to a small extent. For the GLONASS-K satellite, larger changes in the bias and RMS reduction result from using 3-day arc solutions. Here, the bias for the GPS+GLONASS 3-day solution becomes close to the bias of the uncoated GLONASS-M satellites. With regard to the tested solutions, the best fit between GNSS and SLR is found when using 3-day arcs from the GPS+GLONASS combination which is in accordance to the results of the previous section.

SLR residuals provide a valuable estimate of the level of consistency in modeling GNSS and SLR observations. A thorough discussion of remaining systematic differences has to take into account that the computed range residuals depend on the PCOs used for the determination of microwave-based GNSS orbits, the LRA offsets, the coating of the retro-reflectors, station-specific range biases, and the modeling of GNSS orbits including radiation pressure forces and the microwave antenna thrust.

3.4 Orbit and network scale

Modeling the Earth radiation pressure decreases the estimated orbital radius (Rodríguez-Solano et al. 2012a) irrespective of whether the estimated orbit position refers to the

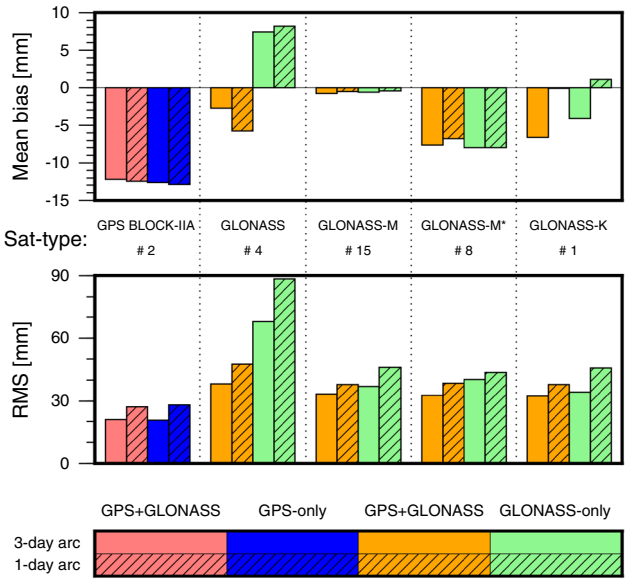

Fig. 9 Validation of microwave-based GNSS orbits using satellite laser ranging (*SLR*). Mean biases (*top*) and RMS (*bottom*) of SLR residuals are separated for satellite types (GPS BLOCK-IIA, GLONASS, GLONASS-M, GLONASS-M*, GLONASS-K), observation combination (GPS+GLONASS, GPS-only, GLONASS-only) and satellite arc length (1 or 3 days). GLONASS-M and GLONASS-M* type retroreflectors are coated and uncoated, respectively (cf. Table 3)

satellite's center of mass or its antenna phase center. In terms of a similarity transformation we need to apply a negative change in scale to satellite positions estimated without modeling this effect in order to fit the positions that have incorporated the albedo modeling. Figure 7 (bottom) shows the results for the scale differences from the seven-parameter similarity transformation of three-dimensional satellite positions. Here, the mean scale difference for the IGS orbits is −0.54 ppb with a discontinuity when switching from reprocessed to operational products on December 30, 2007. Nevertheless, the negative mean scale difference is in accordance to the comparison of our orbit solutions to satellite positions not corrected for albedo and the Earth infrared radiation. The CODE reprocessing series is generated also without modeling the effect of Earth radiation pressure. Compared to our solution this is one of the major modeling differences which leads to negative scale estimates for GPS and GLONASS. The averaged GPS scale difference is found to be −0.74 ppb (19.6 mm at satellite altitude) which corresponds to the radial offset of 1–2 cm for GPS orbits reported by (Rodríguez-Solano et al. 2012). Corresponding scale variations have a period of about 85.5 days ($\approx 1/6$ of the GLONASS draconitic year). The scale difference for GLONASS shows larger variations until end of 2007. Starting with year 2009, its scatter compares well to that obtained for GPS from the IGS orbits. This date coincides with the start of using screened observation files from the operational CODE processing instead of screened observation files resulting from a previous reprocessing run. Although the CODE reprocessing series is also a rigorous combination of GPS and GLONASS, different mean scale offsets are found for both satellite systems. This is potentially due to the fact that antenna thrust is modeled for GPS only.

For GNSS, the scale is conventionally fixed by defining the product of the gravitational constant and the mass of the Earth when modeling orbital dynamics as well as defining the speed of light (McCarthy and Petit 2004; Petit and Luzum 2010). Its realization results from the real signal propagation time in conjunction with the application of observation models for signal delays and antenna PCOs. Absolute receiver antenna PCOs can be derived from ground-based calibration measurements. For satellites, however, corresponding calibration data are missing which makes it necessary to estimate associated values from receiver tracking observations (Schmid et al. 2007). Consequently, satellite antenna PCOs do not only refer to the fixed receiver antenna PCOs and fixed station coordinates. In principle, they are also intrinsically linked to other models applied or omitted during the process of observation reduction. In this regard, we have to pay special attention to the consideration of Earth albedo, because it mainly causes a positive acceleration of the GNSS satellites in radial direction. Here, we introduced satellite antenna PCOs which are consistent with the IGS08 reference frame and have been determined without applying albedo corrections. With a mean positive radial acceleration, unmodeled albedo effects cause associated z-offset values to be overestimated. On the one hand, fixing these biased offsets in our analysis and modeling Earth albedo decreases the scale of the estimated station network. Rodríguez-Solano et al. (2012a) found a scale difference of 0.14 ppb from a comparison of the station positions based on solutions with and without Earth radiation pressure and antenna thrust which can partly explain our scale offset of −2.7 mm (−0.4 ppb) with respect to IGS08 (Table 2). On the other hand, it means that the effect of Earth albedo is overcorrected in our solution which requires a thorough interpretation of the resulting station network scale. However, the scale rate is not affected as modeled albedo variations are limited to annual periods.

3.5 Earth rotation parameters

Figure 10 shows the differences for Earth rotation pole offsets and pole rates from 1- and 3-day GPS+GLONASS combined solutions with respect to the operational IGS solutions. For offset and rate estimates we see a slight smoothing effect in the 3-day solutions compared to the 1-day solutions, which is caused partially by the continuity constraints at the day boundaries and partially due to the longer satellite arcs. In the 1-day solutions the ERPs are estimated without continuity constraints.

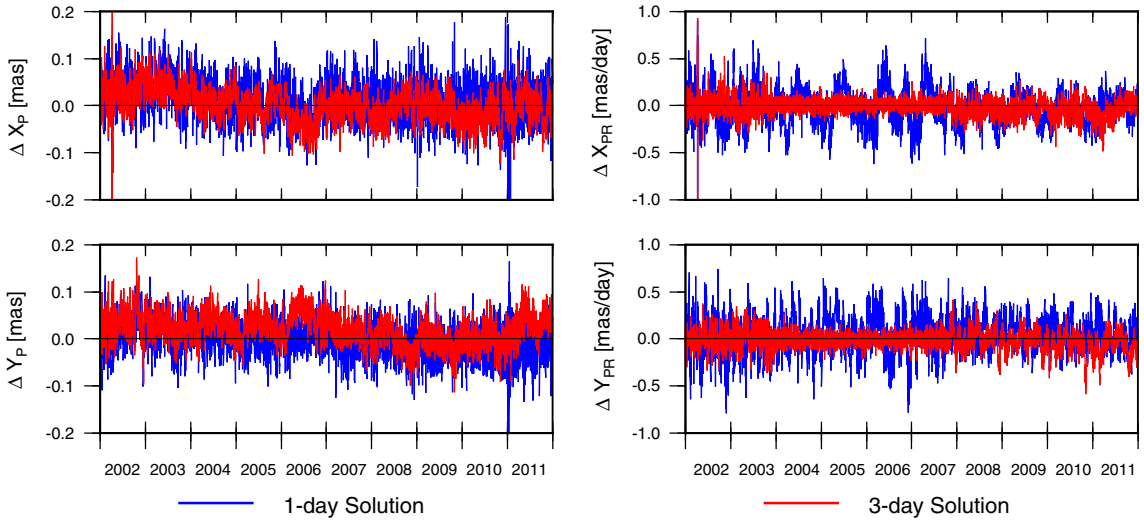

Fig. 10 Comparison of Earth rotation parameter estimates (pole and pole rates) derived from 1-day (*blue*) and 3-day (*red*) GPS+GLONASS combined solutions with respect to the operational IGS series for the period 2002–2011

Table 4 Standard deviations of Earth rotation parameter (ERP) estimates from different types of 1-day GNSS solutions with respect to the operational IGS daily series

ERPs	Unit	GLONASS-only		GPS-only		GPS+GLONASS combined	
		2002–2011	2010	2002–2011	2010	2002–2011	2010
X_P	mas	0.0528	0.0457	0.0508	0.0455	0.0508	0.0456
Y_P	mas	0.0400	0.0359	0.0382	0.0362	0.0382	0.0362
X_{PR}	mas/day	2.8761	0.5648	0.1908	0.1449	0.1892	0.1421
Y_{PR}	mas/day	3.1069	0.6570	0.2050	0.1633	0.2016	0.1523

The GLONASS-only solutions still have a noise level that is about 15 times bigger for the pole rates compared to the GPS-only and the GPS+GLONASS combined solutions from 2002 to 2011 (see Table 4). The GPS+GLONASS combined solutions are only marginally better than the GPS-only solutions. The differences between the GPS-only, GLONASS-only and the combined solutions are shown in the left and right column of Fig. 11. We see that the differences between the GLONASS-only and the combined solutions are much bigger than those between the GPS-only and the combined solutions, especially for the years before 2004. Because of the increasing number and influence of the GLONASS satellites in the course of these 10 years, the differences between GPS-only and combined solutions are getting larger, while the differences between GLONASS-only and combined solutions are decreasing.

3.6 GNSS satellite clocks

Computing the modified Allan deviation (MDEV, Riley 2008) as a measure of frequency stability, we evaluate the performance of our high-rate (30 s) GPS and GLONASS satellite clocks derived from the code+phase solution. Figure 12 shows the results computed from the first 5-day interval in 2008 (different for each satellite) in which only few epochs were missing (<5 % for GPS and <15 % for GLONASS). After removing an offset and drift for each day, we align consecutive daily series using the common midnight epoch. In principle, phase-only clock estimates are of high quality over short periods of time. However, if new ambiguities need to be introduced because of missing observations or receiver tracking problems, consecutive clock estimates reveal jumps and cannot be aligned with respect to each other. Similar jumps may also appear in a code+phase solution depending on the noise of the code and the intervals between such events.

In terms of the MDEV, our GPS satellite clock results are consistent with those from Senior et al. (2008). Periodic variations evident from Fig. 12 (especially for BLOCK-II/IIA) have also been reported by other authors, e.g., for the 3, 4, 6 and 12 h harmonics. Senior et al. (2008) state that a thermal imbalance in the satellite interior is a possible cause for these variations. Clocks on-board GLONASS satellites show a similar performance but no impact due to orbital harmonics like GPS. In comparison to GPS, a larger number of missing epochs prevents a computation of the MDEV for

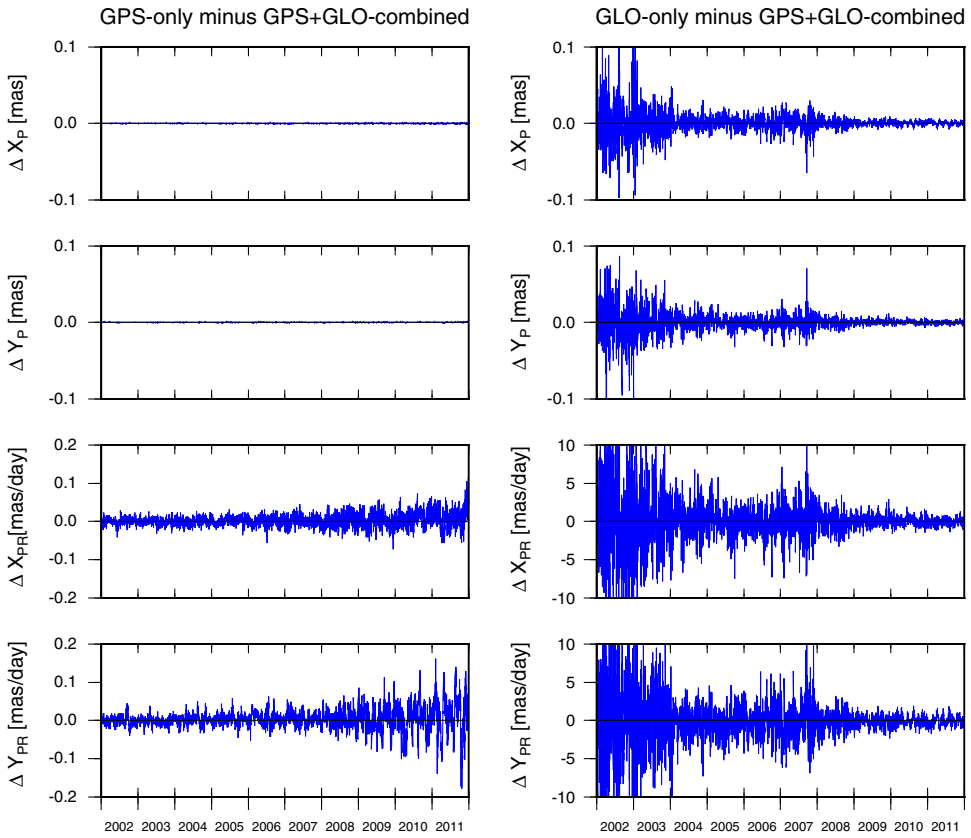

Fig. 11 Differences in Earth rotation pole and pole rate estimates between GPS-only (*left*), GLONASS-only (*right*) solution and GPS+GLONASS combined solution from 1-day solutions

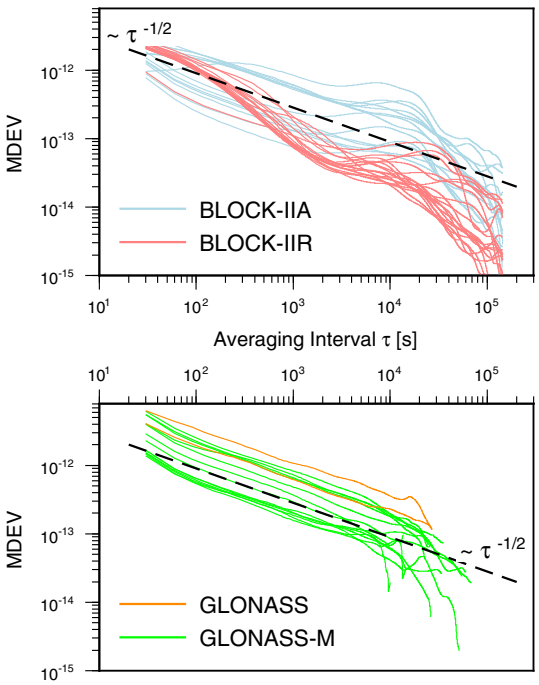

Fig. 12 Modified Allan deviation (*MDEV*) for GPS (*top*) and GLONASS (*bottom*) code+phase satellite clock time series computed from the first 5-day interval in 2008 (different for each satellite) where only few epochs were missing (<5 % for GPS and <15 % for GLONASS)

long averaging intervals. Also, the MDEV from GLONASS reveals a much clearer proportionality to one over square root of the averaging time, indicating that these clock variations can predominantly be characterized as a random walk process.

For an evaluation of the GPS+GLONASS combined clock solution, we fix the estimated GNSS satellite clocks and associated orbits to compute daily coordinates and 2-h tropospheric zenith delays for nearly 90 globally distributed ground tracking stations in a Precise Point Positioning (PPP, Zumberge et al. 1997) mode. Exemplarily, Fig. 13 shows the RMS of PPP phase residuals for each individual satellite. In general, the RMS values are at a 2-mm level which is close to the noise of the microwave phase measurements at zenith both, for GPS and GLONASS. Exceptions are substantial during periods of yaw maneuvers, in particular for those satellites whose navigation antenna is off-centered with respect to the satellite's rotation axis, e.g., the BLOCK-II/IIA and GLONASS-M type satellites.

Phase residuals associated with yaw maneuvers are reported for GPS BLOCK-II and GLONASS-M type satellites by Kouba (2009) and Dilssner et al. (2011), respectively. Here, we only model the nominal yaw attitude. In Fig. 13, satellites with large residuals due to yaw maneuvers are G10, G32 (both BLOCK-IIA) and R07 (GLONASS-M).

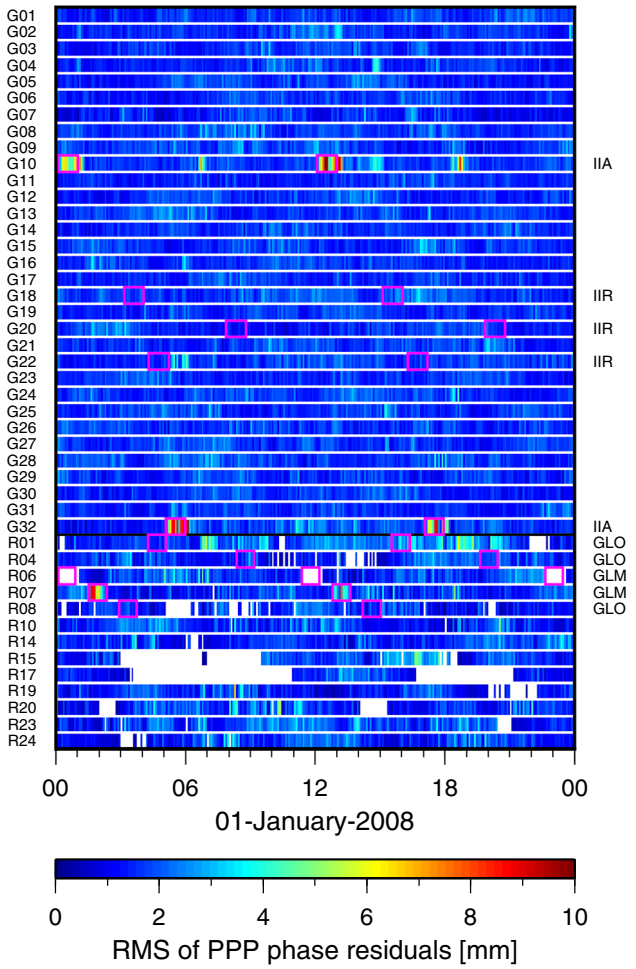

Fig. 13 Root mean square (*RMS*) of Precise Point Positioning (*PPP*) phase residuals for GPS (G) and GLONASS (R) satellites on January 1, 2008. *Pink rectangles* indicate Sun–Earth eclipsing periods. Satellite block types are BLOCK-IIA (*IIA*), BLOCK-IIR (*IIR*), GLONASS (*GLO*) and GLONASS-M (*GLM*)

Moreover, for G10 not only the yaw shadow maneuvers are visible (beginning and middle of the day), but also the yaw noon maneuvers. Other BLOCK-IIR (G18, G20, G22) and GLONASS (R01, R04, R08) satellites also have Sun–Earth eclipses (and possibly perform yaw maneuvers) during this day, but they do not show particularly large residuals. The reason can be found in the zero antenna eccentricity valid for these satellites. Yaw error-induced phase wind-up is fully absorbed by the satellite clock corrections in this case. A different behavior shows R06 (GLONASS-M) which is turned off during the eclipse passages not only for this day, but also for the whole year 2008. From Fig. 13 we also conclude that starting from 2008 the network of GLONASS-tracking ground stations achieves global coverage which allows us to derive corresponding satellite clocks almost without interruptions.

4 Conclusions

The use of GPS and GLONASS in a combined solution provides a larger amount and better coverage of GNSS observations. However, the contribution of each GNSS strongly depends on the number of tracking network sites and satellites in the constellation. In this regard, GLONASS contributes only to a small extent until the end of 2007 as compared to the amount of data available from the global GPS network. Nevertheless, the use of additional GLONASS observations clearly shows an improvement of the repeatability of daily station positions. No systematic differences could be identified for the long-term station positions and velocities between the GPS-only and combined GPS+GLONASS solutions.

In general, the quality of microwave-derived GLONASS orbits improves when combining with GPS. This becomes obvious from both, the orbit overlaps showing the internal precision and the SLR residuals that indicate the external accuracy with independent measurements. If only a small number of observations is available due to a sparse tracking network, GLONASS orbits can be improved significantly by forming 3-day arcs instead of using daily observations only.

Due to the GPS orbital period of approximately half a siderial day, the groundtrack of GPS satellites is nearly unchanged from day to day. In combination with the sparse SLR network the corresponding observations are distributed inhomogeneously. At particular times of the day, the satellites are always observed by the same stations or not observed at all in case of a lack of SLR stations. As opposed to GPS, the groundtrack of GLONASS satellites varies on much shorter time scales which leads to a more regular distribution of SLR observations (Fig. 8).

We find a remarkable improvement of mean SLR biases in the validation of GNSS satellite orbits. The mean SLR bias is −12.2 and −3.2 mm for GPS and GLONASS satellites, respectively. A slightly larger bias is observed for GLONASS-M satellites with uncoated retro-reflectors (−7.6 mm) as compared to the GLONASS-M with coated retro-reflectors (−0.8 mm). The biases are reduced with respect to previous studies due to an appropriate modeling of Earth radiation pressure (including the infrared portion), satellite antenna thrust, and due to correcting for the atmospheric non-tidal loading at the observation level (reducing the Blue-Sky effect).

We present first results of a combined GPS+GLONASS clock solution. The behavior of GPS and GLONASS satellite clocks conforms to the expectations and shows that GLONASS satellite clocks can be almost continuously computed starting at 2008. Data gaps in the GLONASS satellite clocks series should reduce as the gaps in the ground tracking network are reduced in the subsequent years. Furthermore, the validation of the clock solution by means of PPP shows

the high fidelity of the models used, with exception of the yaw maneuver periods which are not yet properly modeled. PPP phase observation residuals are found to be at the level of 2 mm, close to the noise of microwave phase measurements at zenith.

Modeling Earth radiation pressure and antenna thrust has been shown to have a significant impact on the realized scale of the global station network and the satellite positions. Consequently, the different consideration of this effect by the various IGS ACs is a limiting factor for the combination of the AC products. Here, the application of a conventional model is required in order to minimize inter AC scale differences.

The contribution of GLONASS becomes considerable starting with the year 2008. Before, the quality of GLONASS-only solutions is rather poor due to a sparse tracking network and the incomplete satellite constellation. Our findings are of particular relevance in view of other GNSS which are currently under construction like the European Galileo and the Chinese BeiDou. Over a short or medium term, the analysis of these upcoming satellite systems faces the challenges associated with a minimum tracking network and a steadily growing satellite constellation. In this regard, our results serve as examples for these future projects.

Acknowledgments The IGS and ILRS are acknowledged for providing the high-quality GNSS and SLR data. The authors would like to thank the Swiss National Science Foundation and the Deutsche Forschungsgemeinschaft for the financial support within the project "Geodätische und geodynamische Nutzung reprozessierter GPS-, GLONASS- und SLR-Daten" (DFG Projects DI 473/39-1 and HU 1558/1-1, SNF Projects 200021E-131228 and 200021E-129032). The comments of the anonymous reviewers were highly appreciated.

References

Altamimi Z, Collilieux X, Métivier L (2011) ITRF2008: an improved solution of the international terrestrial reference frame. J Geod 85(8):457–473. doi:10.1007/s00190-011-0444-4

Amiri-Simkooei AR (2013) On the nature of GPS draconitic year periodic pattern in multivariate position time series. J Geophys Res 118(5):2500–2511. doi:10.1002/jgrb.50199

Beutler G, Brockmann E, Gurtner W, Hugentobler U, Mervart L, Rothacher M, Verdun A (1994) Extended orbit modeling techniques at the CODE processing center of the International GPS service for geodynamics (IGS): theory and initial results. Manuscr Geod 19(6):367–386

Bizouard C, Gambis D (2009) The combined solution C04 for earth orientation parameters consistent with international terrestrial reference frame 2005. In: Drewes H (ed) Geodetic reference frames, vol 134. IAG Symp, Munich, Germany, p 265–270, doi:10.1007/978-3-642-00860-3_41

Blewitt G (2003) Self-consistency in reference frames, geocenter definition, and surface loading of the solid Earth. J Geophys Res 108(B2). doi:10.1029/2002JB002082

Bock H, Dach R, Jäggi A, Beutler G (2009) High-rate GPS clock corrections from CODE: support of 1 Hz applications. J Geod 83(11):1083–1094. doi:10.1007/s00190-009-0326-1

Böhm J, Werl B, Schuh H (2006) Troposphere mapping functions for GPS and very long baseline interferometry from European centre for medium-range weather forecasts operational analysis data. J Geophys Res 111:B02406. doi:10.1029/2005JB003629

Chen G, Herring TA (1997) Effects of atmospheric azimuthal asymmetry on the analysis of space geodetic data. J Geophys Res 102(B9):20489–20502. doi:10.1029/97JB01739

Clarke PJ, Lavallée DA, Blewitt G, van Dam TM, Wahr JM (2005) Effect of gravitational consistency and mass conservation on seasonal surface mass loading models. Geophys Res Lett 32:L08306. doi:10.1029/2005GL022441

Dach R, Hugentobler U, Fridez P, Meindl M (2007) Bernese GPS software Version 5.0. Astronomical Institute, University of Bern, Switzerland

Dach R, Brockmann E, Schaer S, Beutler G, Meindl M, Prange L, Bock H, Jäggi A, Ostini L (2009) GNSS processing at CODE: status report. J Geod 83(3–4):353–365. doi:10.1007/s00190-008-0281-2

Dach R, Schmid R, Schmitz M, Thaller D, Schaer S, Lutz S, Steigenberger P, Wübbena G, Beutler G (2011) Improved antenna phase center models for GLONASS. GPS Solut 15(1):49–65. doi:10.1007/s10291-010-0169-5

Dach R, Schaer S, Lutz S, Meindl M, Bock H, Orliac E, Prange L, Thaller D, Mervart L, Jäggi A, Beutler G, Brockmann E, Ineichen D, Wiget A, Weber G, Habrich H, Ihde J, Steigenberger P, Hugentobler U (2012) Center for orbit determination in Europe: IGS technical report, 2011 In: Meindl M, Dach R, Jean Y (eds) International GNSS service: technical report 2011. Astronomical Institute University of Bern, IGS Central Bureau, Bern, p 29–40

Dilssner F, Springer T, Gienger G, Dow JM (2011) The GLONASS-M satellite yaw-attitude model. Adv Space Res 47(1):160–171. doi:10.1016/j.asr.2010.09.007

Dow JM, Neilan RE, Rizos C (2009) The international GNSS service in a changing landscape of global navigation satellite systems. J Geod 83(3–4):191–198. doi:10.1007/s00190-008-0300-3

Eanes RJ, Bettadpur S (1996) The CSR 3.0 global ocean tide model: diurnal and semidiurnal tides from TOPEX/POSEIDON altimetry. Technical memorandum / Center for Space Research, the University of Texas at Austin, Center for Space Research

Flechtner F (2007) AOD1B product description document, GRACE/Level-1 Documentation. http://isdc.gfz-potsdam.de, ftp://podaac.jpl.nasa.gov/allData/grace/docs/AOD1B_20070413

Fliegel HF, Gallini TE, Swift ER (1992) Global positioning system radiation force model for geodetic applications. J Geophys Res 97(B1):559–568. doi:10.1029/91JB02564

Fliegel HF, Gallini TE (1996) Solar force modeling of block-IIR global positioning system satellites. J Spacecr Rockets 33(6):863–866

Flohrer C (2008) Mutual validation of satellite-geodetic techniques and its impact on GNSS orbit modeling. Geodätisch-geophysikalische Arbeiten in der Schweiz 75, ISBN 978-3-908440-19-2

Fritsche M, Döll P, Dietrich R (2012) Global-scale validation of model-based load deformation of the earth's crust from continental water-mass and atmospheric pressure variations using GPS. J Geodyn 59–60:133–142. doi:10.1016/j.jog.2011.04.001

Kouba J (2009) A simplified yaw-attitude model for eclipsing GPS satellites. GPS Solut 13(1):1–12. doi:10.1007/s10291-008-0092-1

McCarthy DD, Petit G (2004) IERS conventions (2003). No. 32 in IERS technical note, IERS Conventions Centre, Frankfurt am Main, Germany

Mendes V, Pavlis EC (2004) High-accuracy zenith delay prediction at optical wavelengths. Geophys Res Lett 31:L14602. doi:10.1029/2004GL020308

Ostini L (2012) Analysis and quality assessment of GNSS-derived parameter time series. Geodätisch-geophysikalische Arbeiten in der Schweiz PhD thesis. http://www.bernese.unibe.ch/publist/2012/phd/diss_lo_4web.pdf

Pavlis EC (2009) SLRF2008: The ILRS reference frame for SLR POD contributed to ITRF2008. Ocean Surface Topography Science Team Meeting, Seattle

Pavlis NK, Holmes SA, Kenyon SC, Factor JK (2012) The development and evaluation of the Earth Gravitational Model 2008 (EGM2008). J Geophys Res 117:B04406. doi:10.1029/2011JB008916

Pearlman MR, Degnan JJ, Bosworth JM (2002) The international laser ranging service. Adv Space Res 30(2):135–143. doi:10.1016/S0273-1177(02)00277-6

Petit G, Luzum B (2010) IERS conventions (2010). No. 36 in IERS Technical Note, Verlag des Bundesamts für Kartographie und Geodäsie, Frankfurt am Main, Germany

Ray RD, Ponte RM (2003) Barometric tides from ECMWF operational analyses. Ann Geophys 21(8):1897–1910. doi:10.5194/angeo-21-1897-2003

Ray J, Altamimi Z, Collilieux X, van Dam TM (2008) Anomalous harmonics in the spectra of GPS position estimates. GPS Solut 12(1):55–64. doi:10.1007/s10291-007-0067-7

Rebischung P, Griffiths J, Ray J, Schmid R, Collilieux X, Garayt B (2012) IGS08: the IGS realization of ITRF2008. GPS Solut 16(4):483–494. doi:10.1007/s10291-011-0248-2

Riley WJ (2008) Handbook of frequency stability analysis. NIST Special Publication 1065, Oakland, USA

Rodríguez-Solano CJ, Hugentobler U, Steigenberger P (2012a) Impact of Albedo radiation on GPS satellites. In: Kenyon S, Pacino MC, Marti U (eds) Geodesy for planet earth, vol 136. IAG Symp, Buenos Aires, Argentina, p 113–119, doi:10.1007/978-3-642-20338-1_14

Rodríguez-Solano CJ, Hugentobler U, Steigenberger P, Lutz S (2012b) Impact of earth radiation pressure on GPS position estimates. J Geod 86(5):309–317. doi:10.1007/s00190-011-0517-4

Rülke A, Dietrich R, Fritsche M, Rothacher M, Steigenberger P (2008) Realization of the terrestrial reference system by a reprocessed global GPS network. J Geophys Res 113:B08403. doi:10.1029/2007JB005231

Savcenko R, Bosch W (2012) EOT11A-Empirical ocean tide model from multi-mission satellite altimetry. DGFI Report No. 89, http://www.dgfi.badw.de/fileadmin/docs/dgfi_reports/DGFI_Report_89.pdf

Schmid R, Steigenberger P, Gendt G, Ge M, Rothacher M (2007) Generation of a consistent absolute phase-center correction model for GPS receiver and satellite antennas. J Geod 81(12):781–798. doi:10.1007/s00190-007-0148-y

Senior KL, Ray JR, Beard RL (2008) Characterization of periodic variations in the GPS satellite clocks. GPS Solut 12(3):211–225. doi:10.1007/s10291-008-0089-9

Sośnica K, Thaller D, Dach R, Jäggi A, Beutler G (2013) Impact of loading displacements on SLR-derived parameters and on the consistency between GNSS and SLR results. J Geod 87(8):751–769. doi:10.1007/s00190-013-0644-1

Springer TA, Beutler G, Rothacher M (1999) A new solar radiation pressure model for GPS. Adv Space Res 23(4):673–676

Steigenberger P, Rothacher M, Dietrich R, Fritsche M, Rülke A, Vey S (2006) Reprocessing of a global GPS network. J Geophys Res 111:B05402. doi:10.1029/2005JB003747

Thaller D, Sośnica K, Dach R, Jäggi A, Steigenberger P (2012) GNSS orbit validation using SLR observations at CODE. Poster presentation at the International GNSS Service Workshop 2012, Olsztyn

Thaller D, Sośnica K, Dach R, Jäggi A, Beutler G, Mareyen M, Richter B (2014) Geocenter coordinates from GNSS and combined GNSS-SLR solutions using satellite co-locations. In: Rizos C, Willis P (eds) Earth on the edge: science for a sustainable planet, vol 139. IAG Symp, Melbourne, Australia, p 129–134. doi:10.1007/978-3-642-37222-3_16

Urschl C, Beutler G, Gurtner W, Hugentobler U, Schaer S (2007) Contribution of SLR tracking data to GNSS orbit determination. Adv Space Res 39(10):1515–1523. doi:10.1016/j.asr.2007.01.038

van Dam TM, Wahr J, Milly PCD, Shmakin AB, Blewitt G, Lavallée D, Larson KM (2001) Crustal displacements due to continental water loading. Geophys Res Lett 28(4):651–654. doi:10.1029/2000GL012120

Weber R, Slater JA, Fragner E, Glotov V, Habrich H, Romero I, Schaer S (2005) Precise GLONASS orbit determination within the IGS/IGLOS pilot project. Adv Space Res 36(3):369–375. doi:10.1016/j.asr.2005.08.051

Willis P, Beutler G, Gurtner W, Hein G, Neilan RE, Noll C, Slater J (1999) IGEX: international GLONASS experiment scientific objectives and preparation. Adv Space Res 23(4):659–663. doi:10.1016/S0273-1177(99)00147-7

Zumberge JF, Heflin MB, Jefferson DC, Watkins MM, Webb FH (1997) Precise point positioning for the efficient and robust analysis of GPS data from large networks. J Geophys Res 102(B3):5005–5017. doi:10.1029/96JB03860